SLAC-PUB-2910
HEPL-906
April 1982
(T/E)

J/ψ RADIATIVE TRANSITIONS TO PSEUDOSCALARS*

Kay C. Königsmann
(Representing the Crystal Ball Collaboration)†
High Energy Physics Laboratory
Stanford University, Stanford, California 94305

and

Stanford Linear Accelerator Center
Stanford University, Stanford, California 94305

ABSTRACT

The Crystal Ball detector at SPEAR is used to study radiative decays of the J/ψ into the pseudoscalars axion, Higgs, π^0, η, η', ι, η_c and η_c'. The absence of any signal for axion and Higgs yields stringent upper limits on their production. The branching ratios for π^0, η, η', η_c and η_c' are found to be consistent with theoretical expectations. Two new states, $\iota(1440)$ and $\theta(1640)$ (the latter being most likely a tensor particle) have been uncovered in the final states $K\bar{K}\pi^0$ and $\eta\eta$, respectively. The theoretical interpretations favor a glueball and four-quark state, respectively.

(Invited talk presented at the XVIIth Rencontre de Moriond: Workshop on New Spectroscopy, Les Arcs, France, March 20-26, 1982.)

---

* Work supported in part by the Department of Energy, contract DE-AC03-76SF00515 and by the National Science Foundation, contract PHY81-07396.

1. INTRODUCTION

It has been argued recently[1] that the physics of scalar particles may well be the number one problem for elementary particle physics today. Our only experimental evidence for such scalars is the massiveness of the gauge bosons and fermions.[2] Therefore, it is imperative to search for any signs of scalar particles, in the low energy as well as the high energy range accessible to experiments. In view of these considerations we have searched for the axion and the Higgs bosons, both particles being due to the breaking of symmetries of the underlying gauge theory. Both searches have been negative, placing stringent limits on production in radiative J/ψ decays and/or their decay modes.

Our second class of J/ψ decays investigated concerns the lowest lying pseudoscalar nonet. This the π^0, η, η' and K particles comprising multiplet is well known to show strong mixing between non-strange and strange flavors.[3] The reason for this strong mixing has been explained[4] within QCD by annihilation of the $\bar{q}q$ system into gluons. By additionally adding a small charm - anticharm ($c\bar{c}$) contribution to these lowest lying pseudoscalars, the unexpectedly large branching fraction for $J/\psi \to \gamma\eta$ and η' with respect to $J/\psi \to \gamma\pi^0$ can be easily explained.[5]

Another field of extreme interest concerns of the existence of gluonium states, also called glueballs. It is hard to conceive a method whereby Quantum-Chromo-Dynamics (QCD) could produce the observed spectrum of $\bar{q}q$ states yet avoid a spectrum of gluonic states. Again, two of the low mass states expected[6] turn out to be scalars: $M(0^{++}) \simeq 1$ GeV and $M(0^{-+}) \simeq 1.3$ GeV. In addition higher excited gluonium scalars are expected above 1.5 GeV. The prime channel to look for glueballs is in J/ψ radiative decays. Glueballs should appear with large branching fractions of order $\mathcal{O}(1 \times 10^{-2})$. The Crystal Ball group has found two new states in radiative J/ψ decays: $\iota(1440)$ and $\theta(1640)$ in the exclusive final states $K\bar{K}\pi^0$ and $\eta\eta$, respectively. Educated guesses favor the glueball alternative for the ι, whereas the θ seems to be a four-quark ($q\bar{q}q\bar{q}$) state.

Two long sought after pseudoscalars of the charmonium model are the $^1S_0(c\bar{c})$ states, the $\eta_c(2980)$ and $\eta_c'(3590)$. Both states have been discovered by the Crystal Ball Collaboration in J/ψ and ψ' inclusive photon transitions. With only one missing $c\bar{c}$-bound state[7] (the $^1P_1$) the QCD inspired charmonium picture is understood very well, only a few predictions still causing headaches.

The success of QCD and the underlying gauge symmetry gives us confidence that we are proceeding in the right direction towards a unified gauge theory.

2. CRYSTAL BALL

The Crystal Ball detector is a device which, in many ways, is ideally suited for the study of transitions between and radiative decays of $\bar{c}c$ states. Details of this detector have been described elsewhere,[8] so let me restrict myself to those characteristics of the detector pertinent to the physics analysis described below. Figure 1 shows an abstract representation of the main components of the Crystal Ball detector. To allow for high resolution measurements of the energy and direction of electromagnetically showering particles ($e^{\pm},\gamma$) over a large solid angle, 672 NaI(Tℓ) crystals (of 20 radiation lengths) are used covering 93% of 4π steradians in the central detector. An additional 60 crystals in the endcap region increase the total solid angle covered to 98% of 4π ster. The energy resolution obtained for photons and electrons is $\sigma_E/E = 2.6\%/(E\ (\mathrm{GeV}))^{1/4}$, its angular resolution varies between 1° and 2°, depending on the energy of the particle. In addition, two magnetostrictive spark chambers and one multiwire proportional chamber around the beam pipe are utilized to tag charged particles. There is no magnetic field and the energy/momentum of hadrons interacting in the (one interaction length of) NaI cannot be determined directly.

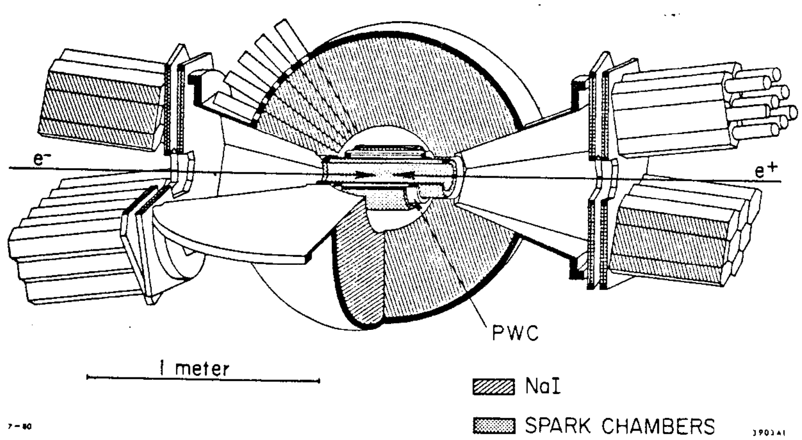

Fig. 1. Schematic of Crystal Ball detector.

3. EVENT SELECTION

The data selection from the raw trigger events to the final physics data sample requires several discrete steps of data reduction. The first step, which yields hadronic resonance events, has been described in detail by F. Porter;[9] we obtain:

$$J/\psi : \int \mathscr{L}\, dt = 765\ \mathrm{nb}^{-1} \quad ; \quad N_{\psi} = 2.2\times 10^{6} \pm 5\%$$

$$\psi' : \int \mathscr{L}\, dt = 3450\ \mathrm{nb}^{-1} \quad ; \quad N_{\psi'} = 1.8\times 10^{6} \pm 5\% \quad .$$

The data sample for the axion search had to be prepared specially as those events do not classify as hadronic events. Furthermore, we require for all tracks $|\cos\theta| \leq 0.90$ (θ is the angle between each track and the incident positron direction) and in addition we cut on the angle between any two tracks: $\cos\theta_{i,j} \leq 0.90$, removing effectively events with spurious photons near hadronic interacting particles.

Finally, we sometimes require photons to have a lateral shower energy deposition in the NaI consistent with that expected from a single electromagnetically showering particle. In the case of a completely determined final state we fit the events kinematically[10] to the required hypothesis. This also eliminates events with a wrong hadron-mass assingment.[11] Additional constraints on the event (e.g., $\eta \to \gamma\gamma$) are utilized. To determine the number of events and the width the signal is fit using MINUIT.[12] The assumed line shape is a Breit-Wigner resonance folded with a Gaussian for resolution.

To determine a branching fraction we need to know the detection efficiency for the particular final state. This was obtained by propagating kinematically generated events through the Crystal Ball detector geometry using the EGS[13] and HETC[14] routines. The main assumption of this procedure is that the pattern of the produced showers and hadronic interactions is close enough to reality. This has been checked thoroughly and found to be correct. To take into account photon conversion in the chambers and beam pipe a correction factor of 1.028 per photon is applied.

All results will have attached to them their statistical and their systematic errors (except upper limit results, where both errors are incorporated in the result). The systematic error arises mainly from the uncertainty in the Monte Carlo simulation of the event.

4. THE AXION AND THE HIGGS

A new pseudoscalar particle, dubbed the axion, has now been with us since 1977 when Peccei and Quinn showed[15] that by adding an extra chiral U(1) symmetry to the total Lagrangian, large P and CP violations of the strong interactions can be remedied. After symmetry breaking the $U(1)_{PQ}$ yields a neutral boson, the axion.[16]

Experimental results on axion production and/or decay have been controversial, either observing[17] the decay of an axion-like particle of mass $m_a \simeq 250$ keV, or ruling out[18] the existence of a standard axion [i.e., one with mass $m_a \simeq \mathcal{O}$(few hundred) keV and a long lifetime $\tau_{a\to\gamma\gamma} \simeq \mathcal{O}(10^{-2\pm2})$ sec].

A major complication in comparing theoretical predictions with experimental results is due to the appearance of an a priori unknown factor x in most predictions. This free parameter is the ratio of the two vacuum expectation values of the two Higgs fields in the theory.

In this experiment we test the axion hypothesis by probing its direct coupling with heavy quarks. The branching ratio for the axion in radiative decays is calculated quite reliably:[19]

$$\frac{B(J/\psi \to \gamma a)}{B(J/\psi \to \mu^+\mu^-)} = \frac{G_F\, m_c^2\, x^2}{\sqrt{2}\,\pi\,\alpha}$$

where G_F is the Fermi coupling constant, m_c the current mass of the charmed quark, and x is the free parameter discussed above. Using[20] $m_c = 1.5 \pm 0.3$ GeV and the experimentally determined branching ratio[3] $B(J/\psi \to \mu\mu) = 0.07 \pm 0.01$, we obtain the following prediction:

$$B_{th}(J/\psi \to \gamma a) = (5.7 \pm 1.4) \times 10^{-5}\, x^2 \quad .$$

As the standard axion does not decay in the detector, we search for events with only one photon of near beam energy. The result[21] of 454 events is displayed in Fig. 2. The hardware trigger threshold was set at 1 GeV. No significant bump is seen above 1 GeV. The scatter plot of Fig. 3(a) explains the cosmic origin of most events: the density of events is highest close to the vertical axis ($\cos\alpha \simeq 1$). Using the lower half of the detector only ($\cos\alpha < 0$), we determine from the absence of any signal [Fig. 3(c)]:

$$B_{exp}(J/\psi \to \gamma a) < 1.4 \times 10^{-5} \qquad (90\%\ \text{C.L.})$$

for any non-interacting, long-lived, pseudoscalar or vector particle.

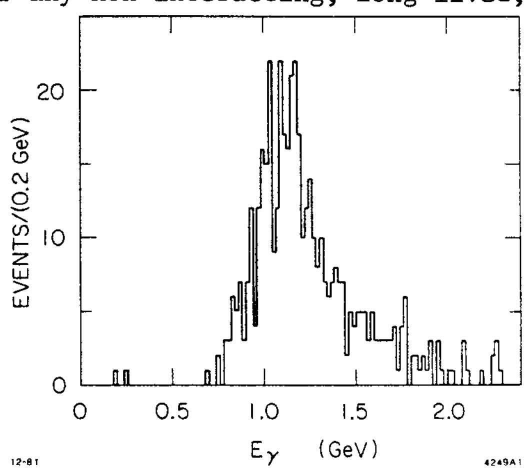

Fig. 2. Photon energy distribution for all one-photon events.

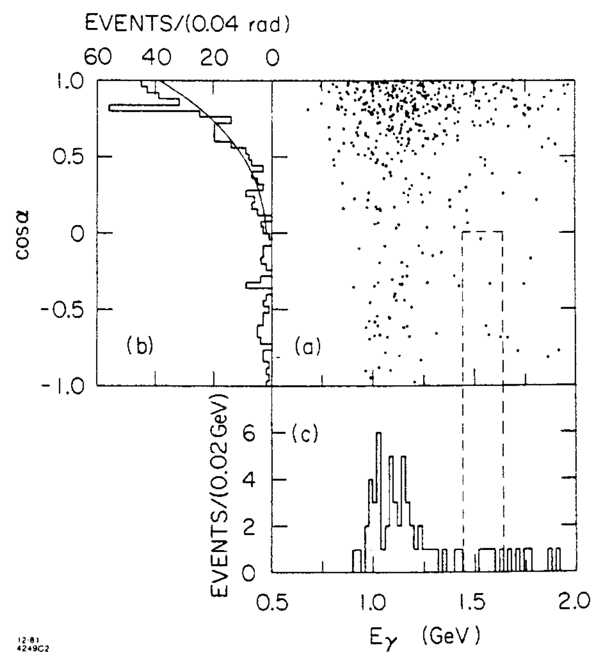

Fig. 3. (a) Scatter plot of photon energy vs cosα, where α is the angle between each track and the vertical axis. The dashed rectangle indicates the ±2σ window for the resolution of photons with beam energy. (b) Distribution of cosα for all one-photon events. The solid curve shows the expected distribution for cosmic-ray events: $dN/d\cos\alpha \propto \text{const} + \cos^2\alpha$, for $\cos\alpha > 0$. (c) Photon energy distribution with $\cos\alpha < 0$; i.e., events in the lower hemisphere of the Crystal Ball.

Comparing our result with the theoretical prediction gives an upper limit on the free parameter x:

$$x < 0.6 \qquad (90\%\ \text{C.L.}) \quad ,$$

in contrast to the value $x = 3.0 \pm 0.3$ cited by the Aachen group.[17] To eliminate the x-dependence of the theoretical prediction a test has been proposed[22] in the simultaneous search for $J/\psi \to \gamma a$ and $\Upsilon \to \gamma a$. Our present result implies that a sensitivity for $\Upsilon \to \gamma a$ of only 10^{-3} will be sufficient to complete this test. The CUSB group at CESR and the LENA group at DORIS have looked[23] for the decays $\Upsilon'' \to \gamma a$ and $\Upsilon \to \gamma a$, respectively. From the absence of any signal in more than 60,000 Υ'' decays (7000 Υ decays) I conclude that the axion seems to be ruled out within the standard model.

Thus we will have to retreat to an even more elusive axion.[24] One that emerges from the symmetry at a very high mass scale, preferably the unification mass in a grand unified theory. Such an axion couples even more weakly to matter and is very light, hence nearly unobservable.

To apply our experimental result to the Higgs boson requires some additional information. The standard Weinberg-Salam theory[25] provides a calculable lifetime and estimates on branching fractions. In order to apply our upper limit to the production of a Higgs in radiative J/ψ decays, we have to ascertain that the Higgs does not decay, which is true for $M_H < 50$ MeV. The theoretical prediction for $B(J/\psi \to \gamma H)$ is identical to the one for axion production with $x = 1$. Therefore, we can rule out[26] any Higgs boson with mass less than 50 MeV. It should be noted here, however, that in the standard W.S. model the Higgs mass[27] appears to be bound by requirements on the stability of the vacuum and the validity of perturbation theory to 7 GeV $\le M_H \le$ 1 TeV. But it has been argued,[28] that a realistic model requires two Higgs doublets, thus removing any constraint on its mass. Light Higgs bosons from those models are ruled out with the result given above.

In view of those models we have also searched for a Higgs boson decaying into $\mu^+\mu^-$ with mass less than 3 GeV. Figure 4 shows the invariant $\mu^+\mu^-$-mass for events satisfying a 2 constraint (2C) fit $J/\psi \to \gamma\mu\mu$. From the absence of any signal we set an upper limit:

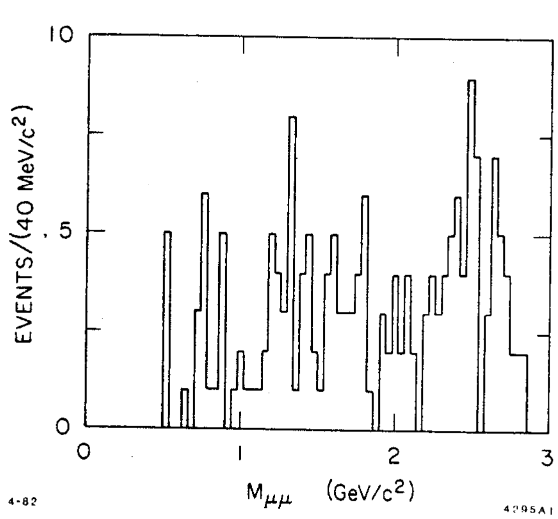

Fig. 4. Invariant $\mu\mu$-mass distribution for events consistent with the hypothesis $J/\psi \to \gamma\mu^+\mu^-$.

$$B(J/\psi \to \gamma H) \times B(H \to \mu^+\mu^-) < \frac{2.4 \times 10^{-5}}{\varepsilon(M_{\mu\mu})} \qquad (90\%\ \text{C.L.})$$

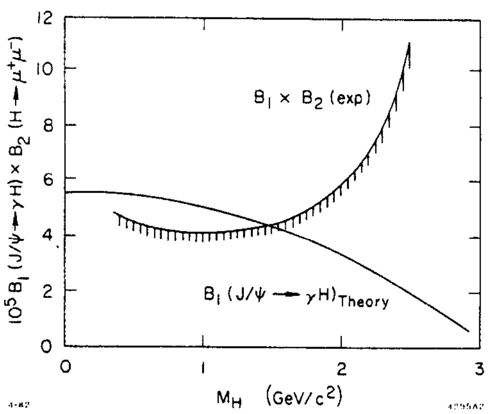

Fig. 5. Experimental upper limit for $J/\psi \to \gamma H$, $H \to \mu^+\mu^-$. The theoretical curve shows $J/\psi \to \gamma H$ only.

for 400 MeV $\le M_H \le$ 3.0 GeV, where the function $\varepsilon(M_{\mu\mu}) = 0.41 + 0.32\ M_{\mu\mu} - 0.16\ M^2_{\mu\mu}$ ($M_{\mu\mu}$ in GeV) describes the total detection efficiency. Figure 5 pictures this upper limit together with the theoretical prediction[29] for $J/\psi \to \gamma H$. As the branching fraction $H \to \mu^+\mu^-$ is very uncertain $\mathcal{O}$(1 to 30)%, our result is not significant enough to rule out massive Higgs bosons.

5. THE PSEUDOSCALAR MESONS π^o, η, η'

Using vector-meson-dominance (VMD) we can relate[30] the following decay widths:

$$\Gamma(J/\psi \to \gamma\pi^o) \simeq \frac{1}{3}\left(\frac{e}{f_\rho}\right)^2 \Gamma(J/\psi \to \pi^o\rho^o) \simeq 1\ \text{eV} \quad .$$

With the η being mainly SU(3) octet and the η' SU(3) singlet (the octet-singlet mixing angle being $\theta = 11^o$) we furthermore expect:[30]

$$R = \frac{\Gamma(J/\psi \to \gamma\eta')}{\Gamma(J/\psi \to \gamma\eta)} \simeq \left(\frac{k_{\eta'}}{k_\eta}\right)^3 \cot^2\theta \simeq 25$$

and

$$\Gamma(J/\psi \to \gamma\eta) \simeq \frac{1}{3}\,\Gamma(J/\psi \to \gamma\pi^o)$$

where $k_{\eta,\eta'}$ is the momentum of the radiated photon. Therefore, due to the SU(3) singlet nature of the J/ψ, we expect about equal radiative decays into π^o and η with branching fractions $\mathcal{O}(1 \times 10^{-5})$, and an enhancement of ~25 for the radiative transition to the η': $B(J/\psi \to \gamma\eta') \simeq \mathcal{O}(1 \times 10^{-3})$.

We can furthermore use the framework of the quark-gluon theory of hadrons (QCD) to introduce[5] a three gluon annihilation term to the mass-matrix of pseudoscalar mesons. Substantial breaking of SU(3) arises from $\mathcal{O}(1\%)$ contributions of η and η' to the η_c. This mixing lowers the ratio to $R \simeq 3.9$ and yields

$$B_{th}(J/\psi \to \gamma\eta) \simeq 0.9 \times 10^{-3}$$
$$B_{th}(J/\psi \to \gamma\eta') \simeq 3.5 \times 10^{-3} \quad .$$

The width into $\gamma\pi^o$ stays small. These predictions agree with earlier experimental results.[31),32)] In order to allow for a more accurate comparison with different theoretical models it is of advantage to use a complete set of data from one experiment. In view of this fact we have determined the branching fractions to π^o, η, and η' using their 2γ final states and in addition using the $\gamma\rho^o$ and $\eta\pi\pi$ modes for η'.

(a) $J/\psi \rightarrow \gamma\pi^o$

The π^o in this decay has an energy of 1545 MeV. This corresponds to a minimum $\gamma\gamma$ opening angle of 10^o for the π^o decay. Over 90% of the π^o decays will have opening angles less than 13^o. This means that nearly all π^o's from $J/\psi \rightarrow \gamma\pi^o$ will form one connected region of energy deposited in the Crystal Ball.

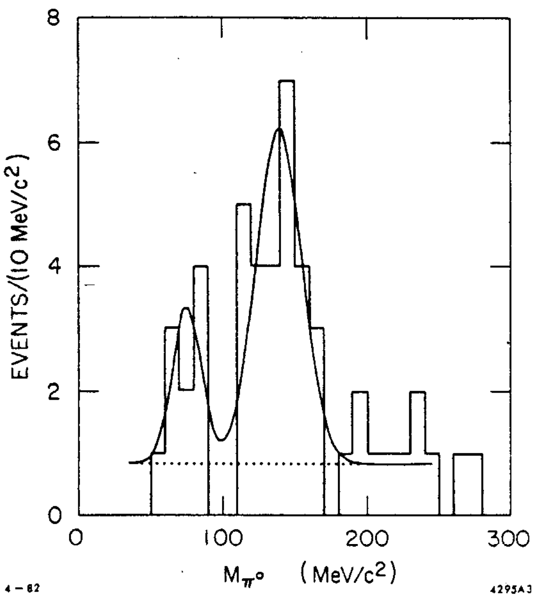

Fig. 6. Distribution of events which satisfy the hypothesis $J/\psi \rightarrow \gamma\pi^o$. See the text for further information.

Events were selected with cuts described above. A maximum likelihood fit was performed to the hypothesis that two photons produce the observed shower pattern. A mass is calculated under this hypothesis and defines a genuine photon by $M(\gamma\gamma \text{ hypothesis}) < 100$ MeV. Selecting genuine photons for one track we obtain the $\gamma\gamma$ mass-spectrum for $\pi^o\gamma$ candidates (Fig. 6). The data have been fit with a flat background and two Gaussians, one for the π^o signal, the other for γ's surviving previous cuts. A signal of 21.1 ± 5.6 events with an efficiency of 27% yield:

$$B(J/\psi \rightarrow \gamma\pi^o) = (3.6 \pm 1.1 \pm 0.8) \times 10^{-5} \quad .$$

This branching ratio is consistent, within experimental errors, with a previous result by the DASP group.[31)] As discussed above VMD predicts[30)] a value of 1×10^{-5}, close to our result. VMD, which works for the light vector mesons, seems to be a good tool for heavy mesons, too.

(b) $J/\psi \rightarrow \gamma\eta$

The best decay mode of the η in terms of small background and large branching ratio is the mode $\eta \rightarrow 2\gamma$. Events with three photons were selected with the above stated cuts. The result of a 4C kinematical fit is presented in a Dalitz plot in Fig. 7. Clear bands at the masses of the η and η' [$M_\eta^2 = 0.3$ (GeV/c^2)^2;

$M^2_{\eta'} = 0.9\ (GeV/c^2)^2$] are visible. The projection onto the $M^{low}_{\gamma\gamma}$ axis is shown in Fig. 8. The two peaks at the η and η' mass stand out. A fit was made to this spectrum, allowing two Gaussians and variable background. No attempt was made to include hard Bhabha corrections and J/ψ direct decay into three photons. 348(73) events are obtained for the η(η') signal. The corresponding efficiencies are 53% (44%). We obtain

$$B(J/\psi \to \gamma\eta) = (0.88 \pm 0.08 \pm 0.11) \times 10^{-3} \quad ,$$

in agreement with previous experiments.[31)]

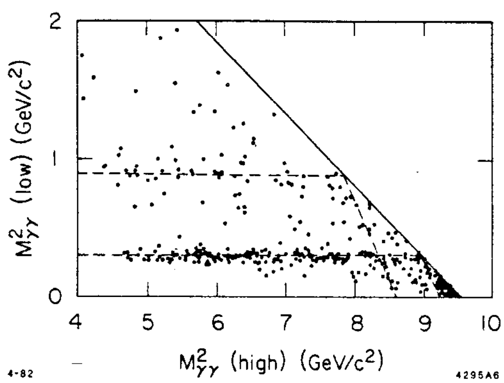

Fig. 7. Dalitz plot for $J/\psi \to \gamma\gamma\gamma$ events.

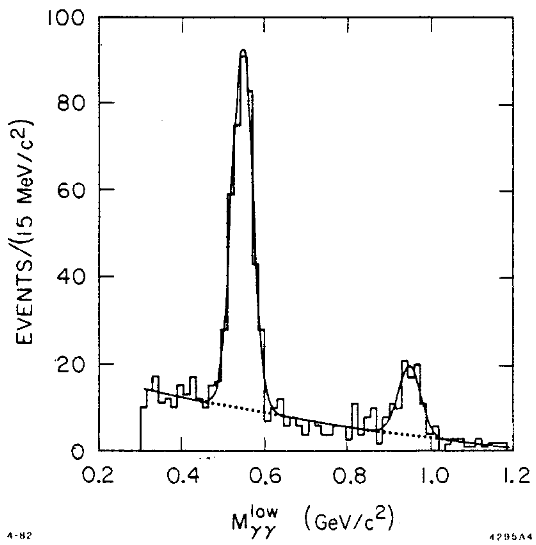

Fig. 8. Projection of the Dalitz plot onto the $M^{low}_{\gamma\gamma}$ axis.

(c) <u>$J/\psi \to \gamma\eta'$</u>

The 73 events observed in Fig. 8 yield a branching ratio

$$B(J/\psi \to \gamma\eta') = (4.4 \pm 0.9 \pm 0.5) \times 10^{-3} \quad (\text{via } \eta' \to \gamma\gamma) \quad .$$

A further check on this result can be obtained by studying the $\gamma\rho^0$ final state of the η'. Events satisfying a 2C fit to the hypothesis $\gamma\gamma\pi^+\pi^-$ were subjected to several more constraints: (i) the high energy neutral track was required to exhibit a shower pattern similar to that expected from genuine photons; (ii) photon pairs forming a π^0 or η were excluded; (iii) the energy of the charged π's had to be less than 1360 MeV; and (iv) the ππ mass should be close to the ρ-mass. These cuts remove the strong $J/\psi \to \pi\rho$ and $J/\psi \to \gamma\eta'$, $\eta' \to \eta\pi^+\pi^-$ background. 666 events in Fig. 9 with an efficiency of 24% yield

$$B(J/\psi \to \gamma\eta') = (4.1 \pm 0.4 \pm 0.6) \times 10^{-3} \quad (\text{via } \eta' \to \gamma\rho^0) \quad .$$

Utilizing the $\eta\pi^+\pi^-$ and $\eta\pi^0\pi^0$ decay modes of the η' we look for events with a topology of three photons two charged or 7(!) photons (we use the 2γ decay of the π^0 and η). Again those events are 3C(7C) fit to the hypothesis $\gamma\eta\pi^+\pi^-$

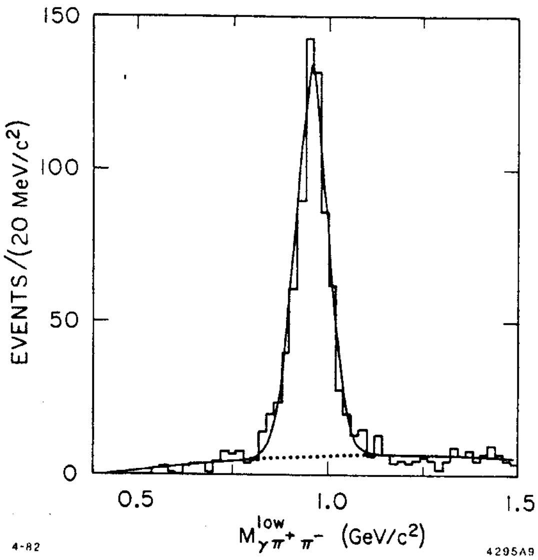

Fig. 9. Distribution of events satisfying the hypothesis $J/\psi \rightarrow \gamma\gamma\pi^+\pi^-$. Cuts on the photon shower distribution and the pion energies have been employed.

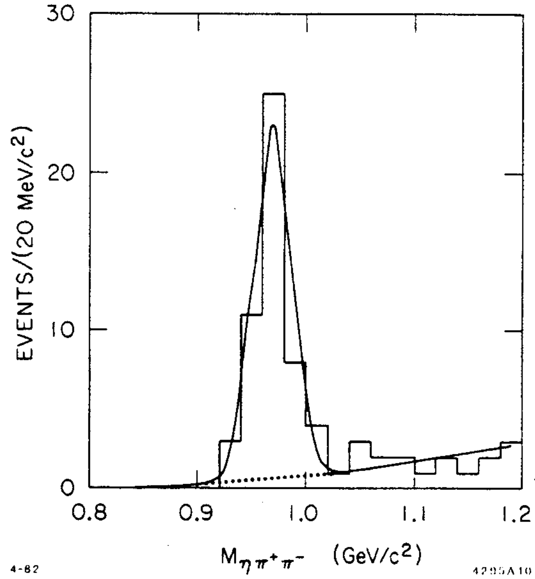

Fig. 10. Distribution for events which are consistent with the hypothesis $J/\psi \rightarrow \gamma\eta\pi^+\pi^-$.

$(\gamma\eta\pi^0\pi^0)$. We observe a clear signal of 48(34) events (Fig. 10 and Fig. 11). The efficiency for detecting such a final state is 3.4% (5.6%), respectively, with $\varepsilon(\eta\pi^+\pi^-)$ being small because of $\gamma\pi^\pm$ overlap problems. The branching ratio is:

$$B(J/\psi \rightarrow \gamma\eta') = (3.9 \pm 1.0 \pm 1.1) \times 10^{-3} \quad (\text{via } \eta' \rightarrow \eta\pi^+\pi^-)$$

$$B(J/\psi \rightarrow \gamma\eta') = (4.2 \pm 0.6 \pm 0.6) \times 10^{-3} \quad (\text{via } \eta' \rightarrow \eta\pi^0\pi^0) \quad .$$

By averaging all four branching ratios we obtain:

$$B(J/\psi \rightarrow \gamma\eta') = (4.1 \pm 0.3 \pm 0.5) \times 10^{-3} \quad (\text{weighted average})$$

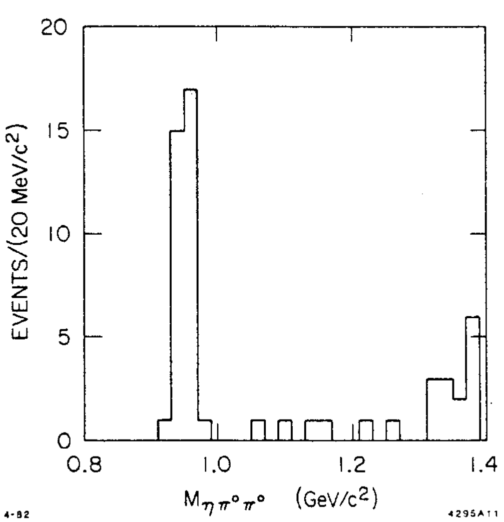

Fig. 11. Distribution for events which are consistent with the hypothesis $J/\psi \rightarrow \gamma\eta\pi^0\pi^0$.

a value slightly higher than that from other experiments,[31] but still consistent within errors. An earlier analysis[32] of half the current data sample yielded, especially for the η', a substantially higher branching ratio. We trace the change to more and better data and to a more accurate photon shower distribution pattern in the Monte Carlo data.

In order to further compare data to theory we calculate:

$$R = \frac{B(J/\psi \rightarrow \gamma\eta')}{B(J/\psi \rightarrow \gamma\eta)} = 4.7 \pm 0.6 \quad .$$

This value can be calculated quite reliably in the context of the 2-gluon annihilation model[5),33)] (independent of the knowledge of overlap integrals) to $R_{th} \simeq 3.9$. A crude estimate for the overlap integrals determines the theoretical branching ratios for η and η' to values close to the measured ones. A second class of theoretical models, based on QCD sum rules, obtain[34)] $R_{th} \simeq 3.7$ and $B(J/\psi \to \gamma\eta) \simeq 1.2 \times 10^{-3}$ by evaluating the matrix element of the gluon field-strength tensor. The latter prediction depends only on the mass of the η and the $\pi \to \mu\nu$ decay coupling constant.

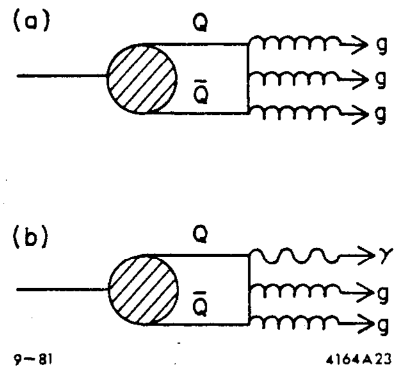

Fig. 12. Leading order QCD diagrams for the decay of the J/ψ into (a) hadrons and (b) a direct photon plus hadrons.

In summary, we can say that the experimental results are in good agreement with predictions from quite different theoretical models. The main similarity between e.g., a potential model and the sum rules is that both rely on the assumption that the radiative decay of the J/ψ proceeds via $c\bar{c} \to$ photon + 2 gluons [Fig. 12(b)] in contrast to the decay into hadrons which proceeds through 3 gluons [Fig. 12(a)]. The total branching fraction into $\gamma + 2g$ is estimated[35)] in lowest order in α_s to:

$$B(J/\psi \to \gamma gg) \simeq \frac{36}{5}\left(\frac{2}{3}\right)^2 \frac{\alpha}{\alpha_s(m_c)} \simeq 10\% \ .$$

Experimentally we can account for less than 1% of the total photonic branching ratio summing over all resonances. The missing 9% could be due either to non-resonant γ + hadron production or the formation of glueballs[4),35)] as intermediate states.

6. TWO NEW RESONANCES: ι(1440) AND θ(1640)

The two gluons in Fig. 12(b) are forced to be a color-singlet because the photon is colorless. Thus the γ potentially samples the gg mass spectrum. But how heavy are bound gluon states[36)] expected to be? Most models like potential models,[37)] bag models,[6),38)] lattice-gauge theories,[39)] and string models[40)] place the lowest lying states $J^P = 0^{++}, 0^{-+}, 2^{++}, 2^{-+}$ at around (1.5 ± 0.5) GeV. In particular within the bag model it is possible to predict[41)] the spin splitting: $M(0^{++}) \lesssim 0$ MeV, $M(0^{-+}) \simeq 1.4$ GeV, $M(2^{++}) \simeq 1.3$ GeV, and $M(2^{-+}) \gtrsim 1.6$ GeV. Estimates based on QCD sum-rules[42)] on the other hand restrict the masses to $M(0^{-+}) \simeq (2\text{–}2.5)$ GeV and $M(2^{++}) \lesssim 2$ GeV. Glueball widths are estimated to be O(10) MeV, with specific predictions being as low as 1 MeV or as high as 100 MeV. So aside from rather uncertain estimates on glueball masses and widths we expect those states (with $M_G < 3$ GeV) to show up in radiative J/ψ decays with branching fractions[43)] of order 1%.

Aside from the known radiative transition to the π^o, η, η', and f the E(1420) had been seen[44] in the final state $K^{\pm}K^o_S\pi^{\mp}$. The Crystal Ball also observes a signal in the decay $J/\psi \to \gamma K^+K^-\pi^o$. Figure 13 shows the $K^+K^-\pi^o$ invariant mass distribution for kinematically fit events. The shaded region is obtained with a low $K\bar{K}$-mass cut $M_{K\bar{K}} \leq 1125$ MeV. A resonance is seen near 1400 MeV which we name the ι (iota). A fit to either distribution yields the following parameters:[45]

$$M_\iota = 1440 \begin{array}{l} +20 \\ -15 \end{array} \text{ MeV} \quad , \quad \Gamma_\iota = 50 \begin{array}{l} +20 \\ -30 \end{array} \text{ MeV}$$

$$B(J/\psi \to \gamma\iota) \times B(\iota \to K\bar{K}\pi) = (4.0 \pm 0.7 \pm 1.0) \times 10^{-3}$$

where the branching ratio has been corrected for all $K\bar{K}\pi$ isospin combinations.

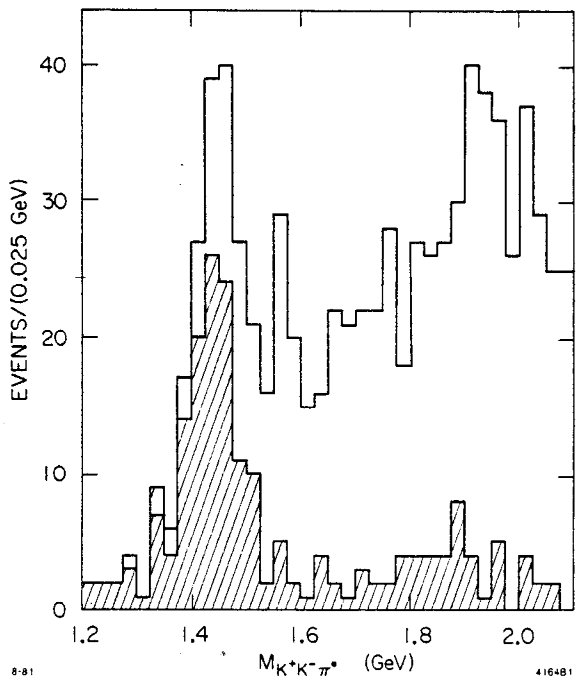

Fig. 13. $K^+K^-\pi^o$ invariant mass distribution for events consistent with the hypothesis $J/\psi \to \gamma K^+K^-\pi^o$. Shaded region has the requirement $M_{K\bar{K}} < 1125$ MeV.

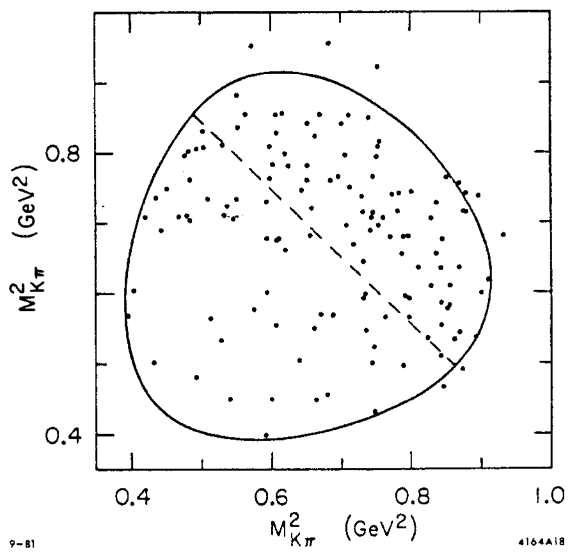

Fig. 14. $K^+K^-\pi^o$ Dalitz plot for events with $1400 \leq M_{K\bar{K}\pi} < 1500$ MeV. Solid curve shows boundary for $M_{K\bar{K}\pi} = 1450$ MeV. Dashed line shows $M_{K\bar{K}} = 1125$ MeV.

Figure 14 shows the Dalitz plot for events with $1400 \leq M_{K\bar{K}} \leq 1500$ MeV. Events seem to cluster in the upper right corner, indicating a low $K\bar{K}$ mass enhancement, which we interpret as evidence for the decay $\iota \to \delta^o(980)\pi^o$ and/or $\iota \to K^*\bar{K} + c.c.$ To determine the relative $\delta\pi/K^*\bar{K}$ contribution and the spin of the ι a partial wave analysis was performed. Ingredients were $K\bar{K}\pi$ phase space, $\delta^o\pi^o$ ($J^P = 0^-$ and 1^+) and $K^*\bar{K} + c.c.$ ($J^P = 0^-$ and 1^+). The significant contributions (corrected for efficiency) are shown in Fig. 15. The $K^*\bar{K} + c.c.$ ($J^P = 1^+$) [Fig. 15(b)] partial wave is relatively small, whereas the $\delta\pi$ ($J^P = 0^-$)

contribution [Fig. 15(c)] shows a clear structure in the ι mass region. We find

$$J^{PC}(\iota) = 0^{-+} \quad \text{and} \quad \frac{B(\iota \to K^*\bar{K} + c.c.)}{B(\iota \to K^*\bar{K} + c.c.) + B(\iota \to \delta\pi)} < 25\% \quad (90\%\ C.L.) .$$

An analysis of the three dimensional angular decay distribution for $J/\psi \to \gamma\iota$, $\iota \to \delta\pi$ determines relative probabilities of 10^{-4} and 8×10^{-3} for spin 1 and 2 relative to spin 0.

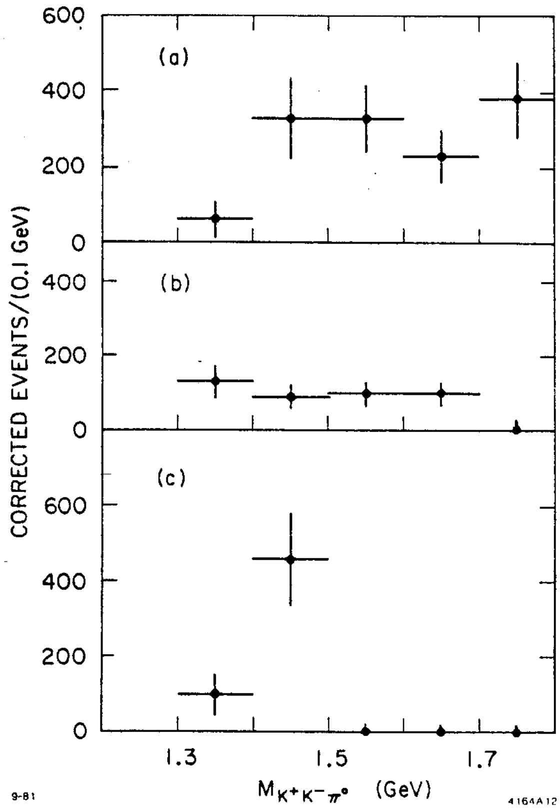

Fig. 15. Partial-wave contributions as a function of $K\bar{K}\pi$ mass for (a) $K\bar{K}\pi$ flat, (b) $K^*\bar{K}$ + c.c. - 1^+, and (c) $\delta\pi$ - 0^-.

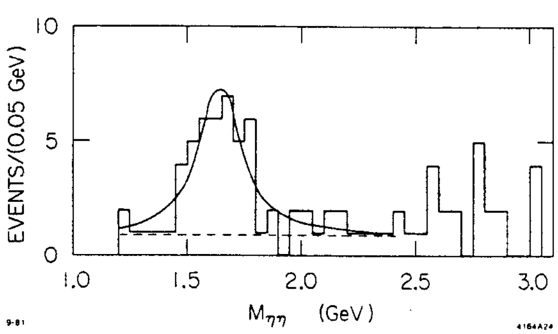

Fig. 16. $\eta\eta$ invariant mass distribution for events which satisfy fits to the hypothesis $J/\psi \to \gamma\eta\eta$. Curve shows result of fit to mass distribution.

It has been suggested by Bjorken[37] that an appropriate scenario of glueball decay suited for the Crystal Ball detector would be glueball $\to \eta\eta$. We have searched for events satisfying a 6C kinematical fit in the final state $J/\psi \to 5\gamma$. The invariant $\eta\eta$-mass is displayed in Fig. 16. A clear signal which we name the θ, emerges with the following parameters

$$M_\theta = 1640 \pm 50 \quad , \quad \Gamma_\theta = 220 {}^{+100}_{-\ 70}$$

$$B(J/\psi \to \gamma\theta) \times B(\theta \to \eta\eta)$$
$$= (4.9 \pm 1.4 \pm 1.0) \times 10^{-4} \quad .$$

Because of limited statistics we cannot exclude a contribution up to 30% from $J/\psi \to \gamma f'$, $f' \to \eta\eta$ to our signal.

We have performed a spin analysis of the θ based on the 3-dimensional angular decay distribution (the polar angle of the photon and the polar and azimuthal angles of one η in the rest frame of the θ). Due to its decay into two pseudoscalars only spin parity 0^+ and 2^+ are allowed (spin 4 or greater is very unlikely). The result of the maximum likelihood fit is shown in Fig. 17. Spin 2 is favored over spin 0 by 2σ, not enough to rule out spin 0 completely.

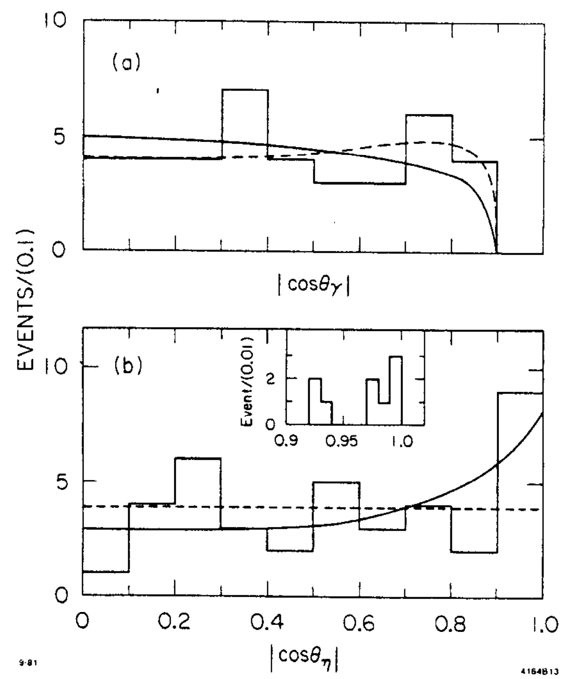

Fig. 17. (a) $|\cos\theta_\gamma|$ and (b) $|\cos\theta_\eta|$ distributions for $J/\psi \to \gamma\theta$, $\theta \to \eta\eta$. Solid curves are best fit distributions for spin 2. Dashed curves are expected distributions for spin 0. Insert shows events with $|\cos\theta_\eta| > 0.9$ with expanded scale.

Both new states have been interpreted as:

- gluonium states[36)-40)]
- radially excited quarkonium states[46)] and
- $q\bar{q}q\bar{q}$ 4-quark states.[47)]

In my opinion the $\iota(1440)$ is almost certainly a glueball. An explanation as a radially excited state suffers from the absence of other strong radiative transitions and a higher mass requirement. The interpretation of ι as a 4q state is easily ruled out by its large branching ratio.

The situation for the $\theta(1640)$ is not so clear: every interpretation given above has been invoked. But not all experimental data can be described satisfactorily by any given model, in particular the non-observation[45),48)] of $\theta \to \pi^+\pi^-$, $K\bar{K}$ raises problems.

To clarify the situation on the ι and θ we should try to accomplish the following tasks:

$\iota(1440)$
- find $\iota \to \eta\pi^+\pi^-$ and $\iota \to \gamma\rho^0$
- find (other) radial excitations e.g., in $J/\psi \to \gamma(0^{-+})^*$
- does $B(\iota \to \delta\pi)/B(\iota \to K^*\bar{K})$ depend on m_ι?
- $B(J/\psi \to \gamma\iota) = ?$
- is the $\delta(980)$ a pure $q\bar{q}$-state or does it have admixtures[49)] from 2-gluon and/or 4-quark states?

$\theta(1640)$
- find $\theta \to \pi\pi$ and $K\bar{K}$
- verify spin 2
- $B(J/\psi \to \gamma\theta) = ?$
- determine $f' \to \eta\eta$ contribution to θ signal
- why is $B(J/\psi \to \gamma f')/B(J/\psi \to \gamma f)$ so small?
- does a $J^{PC} = 2^{++}$ 4q-state exist?
- can a 2-gluon 2^{++} ground-state be heavier[50)] than the first excited state 0^{-+}?

Only with the availability of some or all of the above given tests will we be able to ascertain the gluonium/radial excitation/4 quark interpretation for the ι and θ. The verification of the $\iota(1440)$ state as a gluonium resonance would be of vital importance for QCD which predicts glueballs as a consequence of the self-coupling of the gluon-field.

7. TWO CHARMED PSEUDOSCALAR MESONS η_c AND η_c'

The search for the spin singlet state η_c and η_c' is of great importance to help us understand the spin forces at very short distances. The hyperfine mass-splitting $1^3S_1 - 1^1S_0$ ($M_\psi - M_{\eta_c}$) has been predicted to be around 100 MeV by such different models as nonrelativistic potential models[51] or QCD field-theoretical model.[52] The predictions for $M_{\psi'} - M_{\eta_c'}$ vary around 70 MeV. Radiative branching ratios to these states ($^3S_1 \to \gamma + {}^1S_0$) is estimated to be $\mathcal{O}(1\%)$.

With the doubling of both the J/ψ and ψ' datasets since 1980 we have repeated the analysis of the inclusive photon spectra. Our aim was to obtain better parameters on the η_c state observed earlier.[53],[54] The treatment of the data has been outlined in the introduction above. For a detailed description of the approach see Refs. 9,57. The final inclusive photon spectrum from the ψ' is shown in Fig. 18. The familiar strong photon lines caused by the transitions $\psi' \to \gamma\chi_{0,1,2}$ and $\chi_{1,2} \to \gamma\psi$ dominate the distribution. Two additional small peaks show up at $E_\gamma = 91$ MeV and 638 MeV. The inserts show these two peaks background subtracted. We obtain the following parameters (the parameters for the η_c have been obtained from simultaneous fits to the J/ψ and ψ' inclusive spectra):

	η_c	η_c'
Mass M	2984 ± 5 MeV	3592 ± 5 MeV
Width Γ	12.4 ± 4.6 MeV	< 8 MeV (95% C.L.)
$B(\psi' \to \gamma^1S_0)$	(0.29 ± 0.08)%	(0.2 - 1.3)% (95% C.L.)
$B(J/\psi \to \gamma^1S_0)$	$(1.20 {}^{+0.53}_{-0.35})$%	N.A.

Both mass values are in line with predictions from the two classes of models discussed above. But higher order QCD corrections[55] seem to raise the spin-singlet masses to within 50 (20) MeV of the J/ψ (ψ'). But as the first order correction amounts to 45% it is difficult to predict the point of convergence for the mass values when higher orders are included. Another first order correction which is uncomfortably large (86%) concerns the ratio $\Gamma(^1S_0 \to \text{hadron})/\Gamma(^3S_1 \to \text{hadron})$. This time the prediction for $\Gamma_{tot}(^1S_0)$ is raised to 8 (7) MeV for the η_c (η_c'). For a very detailed comparison of experimental information on the χ and the η_c and η_c' states with different theoretical predictions see Ref. 56.

In addition to the inclusive photon analysis of J/ψ and ψ' we have also repeated[32] the search for the $\eta_c \to \gamma\gamma$ in the $J/\psi \to 3\gamma$ data, which is identical to the analysis presented above for η, $\eta' \to 2\gamma$. Projecting the Dalitz plot

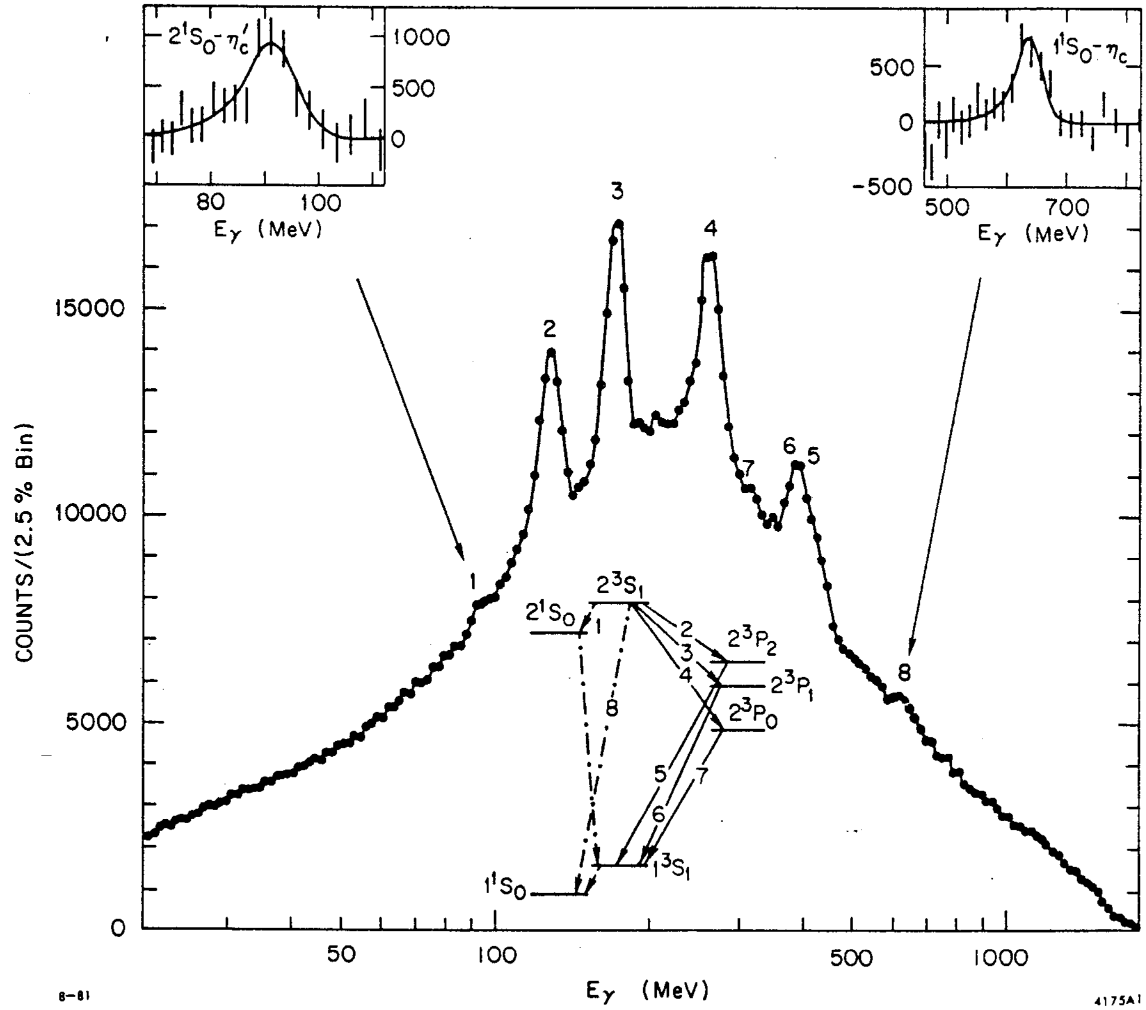

Fig. 18. Inclusive γ-spectrum at the ψ'. The upper inserts show the background subtracted signals for the η_c and η_c' candidate states. The charmonium level scheme is included.

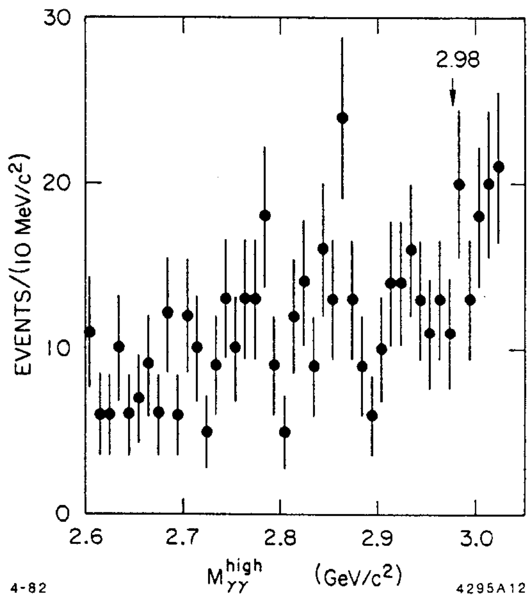

Fig. 19. Projection of the Dalitz plot (Fig. 7) onto the $M_{\gamma\gamma}^{high}$ axis.

(Fig. 7) onto the high mass axis yields Fig. 19. There is no significant signal observed above background. We thus set a limit (for resonances with $\Gamma \lesssim 25$ MeV):

$$B(J/\psi \to \gamma X) \times B(X \to 2\gamma) < 1.6 \times 10^{-5} \quad (90\%\ \text{C.L.})$$

where $2.6 \le M_X \le 3.0$ GeV. Let us apply the result to the η_c and divide out the $J/\psi \to \gamma\eta_c$ branching ratio and multiply by the observed total width. We obtain $\Gamma(\eta_c \to \gamma\gamma) \lesssim 20$ keV, comfortably above model predictions[51),55)] of about 6 keV.

In conclusion, the spectroscopy of heavy quark-antiquark ($c\bar{c}$) systems has been proven to be an enormously fruitful area. The smallness of the scales involved justify a nonrelativistic perturbative approach. Many predictions have been met by experimental results and many experiments gave new guidelines for theoretical investigations. The discrepancy observed between theory and experiment is significant only in the following areas: the total width of the χ and η_c states, and in the decay width $\Gamma(J/\psi \to \gamma\eta_c)$. But, again, higher order QCD corrections may eventually bridge this gap.

REFERENCES

† The Crystal Ball Collaboration: C. Edwards, R. Partridge, C. Peck, F. C. Porter (Caltech); D. Antreasyan, Y. F. Gu, J. Irion, W. Kollman, M. Richardson, K. Strauch, K. Wacker (Harvard); A. Weinstein, D. Aschman, T. Burnett, M. Cavalli-Sforza, D. Coyne, M. Joy, C. Newman, H. Sadrozinski (Princeton); D. Gelphman, R. Hofstadter, R. Horisberger, I. Kirkbride, H. Kolanoski, K. Königsmann, R. Lee, A. Liberman, J. O'Reilly, A. Osterheld, B. Pollock, J. Tompkins (Stanford); E. Bloom, F. Bulos, R. Chestnut, J. Gaiser, G. Godfrey, C. Kiesling, J. Leffler, S. Lindgren, W. Lockman, S. Lowe, M. Oreglia, D. Scharre (SLAC).

1) L. B. Okun, Proc. of the 1981 International Symposium on Lepton and Photon Interactions, Bonn, 1981, ed. by W. Pfeil.

2) We assume here the validity of a renormalizable gauge theory.

3) Particle Data Group, Rev. Mod. Phys. 52, 2 (1980).

4) See e.g., H. Fritsch and P. Minkowski, Nuovo Cimento 30, 393 (1975); A. de Rújula et al., Phys. Rev. D 12, 147 (1975).

5) H. Fritsch and J. D. Jackson, Phys. Lett. 66B, 365 (1977).

6) See e.g., the prediction within the bag model: J. Donoghue, K. Johnson and B. Li, Phys. Lett. 99B, 416 (1981).

7) F. Porter, SLAC-PUB-2881 and Proc. of the XVII Rencontre de Moriond (1982), ed. by Tran Thanh Van, in press.

8) M. Oreglia, Ph.D. Thesis, Stanford Linear Accelerator Center, Stanford University, SLAC-236 (1980), and to be published in Phys. Rev. D, May 1982.

9) F. Porter, Proc. of the Summer Institute on Particle Physics, Stanford ed. by A. Mosher, and SLAC-248 (1981).

10) Kinematical fit routine based on fit 70 by J. C. Parks, SLAC-150, UC-34.

11) Note that the kinematical fit determines the momenta of hadrons for a given mass hypothesis. The distinction between different mass assignments is good for low hadron momenta, i.e., for all the final states considered here.

12) F. James and M. Roos, CERN Computer Center, Library D506 and D516.

13) R. L. Ford and W. R. Nelson, SLAC-210 (1978).

14) Engineering Physics Division, Oak Ridge National Lab, CCC-178.

15) R. D. Peccei and H. R. Quinn, Phys. Rev. Lett. 38, 1440 (1977), and Phys. Rev. D 16, 1791 (1977).

16) S. Weinberg, Phys. Rev. Lett. 40, 223 (1978).

17) H. Faissner, Proc. of the 1981 International Symposium on Lepton and Photon Interactions, Bonn, 1981, ed. by W. Pfeil.

18) D. J. Bechis et al., Phys. Rev. Lett. 42, 1511 (1979); J. L. Vuilleumier et al., Phys. Lett. 101B, 341 (1981); J. Frère et al., ibid, 103B, 129 (1981); M. Wise, ibid, 103B, 121 (1981); A. Zehnder, ibid, 104B, 494 (1981); A. Zehnder, K. Gabathuler and J. L. Vuilleumier, SIN-PR-82-01, to be published in Phys. Lett. B; R. D. Peccei, MPI-PAE/Pth 45/81, and references therein.

19) F. Wilczek, Phys. Rev. Lett. 40, 279 (1978).

20) S. Weinberg, The Problem of Mass, in A Festschrift for I. I. Rabi, ed. by L. Motz, New York, 1978; M. A. Shifman, Proc. of the 1981 International Symposium on Lepton and Photon Interactions, Bonn, 1981, ed. by W. Pfeil.

21) For a complete description see C. Edwards et al., Phys. Rev. Lett. 48, 903 (1982).

22) F. C. Porter and K. C. Königsmann, Phys. Rev. D 25, 1993 (1982).

23) Private communication by P. Franzini, T. Böhringer (CUSB) and M. Coles (LENA).

24) M. Dine, W. Fischler and M. Srednicki, Phys. Lett. 104B, 199 (1981); S. Dimopoulos, S. Raby and F. Wilczek, Phys. Rev. D 24, 1681 (1981); M. B. Wise, H. Georgi and S. L. Glashow, Phys. Rev. Lett. 47, 402 (1981).

25) S. Weinberg, Phys. Rev. Lett. 19, 1264 (1967); A. Salam, Proc. of the Eight Nobel Symposium on Elementary Particle Theory, Stockholm, ed. by N. Svartholm, 1968.

26) A low energy bound ($m_H > 13$ MeV) for Higgs exists from neutron-electron and neutron-nucleus scattering: S. Adler, R. Dashen and S. Treiman, Phys. Rev. D 10, 3728 (1974); R. Barbieri and T. Ericson, Phys. Lett. 57B, 270 (1975).

27) See e.g., A. I. Vainstein, V. I. Zakharov and M. A. Shifman, Usp. Fiz. Nauk. 131, 537 (1980); A. Ali, DESY-81-060, September 1981 and 1981 Isabelle Summer Workshop, Upton, New York 1981.

28) See e.g., G. L. Kane, LM-HE-81-56, September 1981, and Summer School in Theoretical Physics, Les Houches, France, 1981.

29) P. H. Frampton and W. W. Wada, Phys. Rev. D 19, 271 (1979); J. Ellis, M. K. Gaillard and D. V. Nanopoulos, Nucl. Phys. B106, 292 (1976).

30) R. N. Cahn and M. S. Chanowitz, Phys. Lett. 59B, 277 (1975); T. F. Walsh, Lett. Nuovo Cimento 14, 290 (1975).

31) W. Braunschweig et al., Phys. Lett. 67B, 243 (1977); W. Bartel et al., ibid, 66B, 489 (1977) and 64B, 483 (1976); D. L. Scharre, SLAC-PUB-2519.

32) R. Partridge et al., Phys. Rev. Lett. 44, 712 (1980).

33) T. N. Pham, Phys. Lett. 87B, 267 (1979).

34) V. A. Novikov et al., Nucl. Phys. B165, 55 (1980); H. Goldberg, Phys. Rev. Lett. 44, 363 (1980).

35) M. Chanowitz, Phys. Rev. D 12, 918 (1975); S. J. Brodsky et al., Phys. Lett. 73B, 203 (1978).

36) H. Fritzsch and M. Gell-Mann, in Proc. of the XVIth International Conference on High Energy Physics, v. 2, ed. by J. D. Jackson and A. Roberts (National Accelerator Laboratory, Batavia, Illinois, 1973), p. 135; J. D. Bjorken, in Quantum Chromodynamics, ed. by A. Mosher (Stanford, California, 1980), p. 219; J. F. Donoghue, in Experimental Meson Spectroscopy - 1980, ed. by S. U. Chung and S. J. Lindenbaum (AIP, New York, 1981), p. 104; J. F. Donoghue, in High Energy Physics - 1980, ed. by L. Durand and L. G. Pondrom

(AIP, New York, 1981), p. 35; P. M. Fishbane, in Gauge Theories, Massive Neutrinos, and Proton Decay, ed. by A. Perlmutter (Plenum Press, New York, 1981), p. 63.

37) D. Robson, Nucl. Phys. B130, 328 (1977); J. D. Borken, Proc. of the Summer Institute on Particle Physics, Stanford, California SLAC-PUB-2372 and SLAC-224 (1980); J. Coyne, P. Fishbane and S. Meskov, Phys. Lett. 91B, 259 (1980).

38) R. L. Jaffe and K. Johnson, Phys. Lett. 60B, 201 (1976); J. Donoghue, to be published in Comments in Nucl. Part. Phys.

39) B. Berg, Phys. Lett. 97B, 401 (1980); G. Bhanot, ibid, 101B, 95 (1981); H. Hamber and G. Parisi, Phys. Rev. Lett. 47, 1792 (1981); S. Pinsky Proc. of the 17th Rencontre de Moriond, Les Arcs, France, March 1982.

40) B. Skagerstam and A. Stern, Phys. Lett. 97B, 405 (1980).

41) T. Barnes, Z. Phys. C10, 275 (1981); C. B. Thorn, unpublished.

42) V. A. Novikov et al., Nucl. Phys. B191, 301 (1981).

43) K. Koller and T. Walsh, Nucl. Phys. B140, 449 (1978).

44) D. Scharre et al., Phys. Lett. 97B, 329 (1980).

45) C. Edwards et al., SLAC-PUB-2896 (1982).

46) I. Cohen and H. Lipkin, Nucl. Phys. B151, 16 (1979); S. Ono and O. Pène, Phys. Lett. 109B, 101 (1982).

47) R. L. Jaffe, Phys. Rev. D 15, 267 (1977). But note that J. Weinstein and N. Isgur, Phys. Rev. Lett. 48, 659 (1982) argue that, except for S^* and δ, no 4q states are stable.

48) D. L. Scharre, in Experimental Meson Spectroscopy - 1980, ed. by S. Chung and S. Lindenbaum (AIP, New York, 1981), p. 329.

49) N. Törnqvist, HU-TFT-82-1 (1982).

50) T. Barnes, F. Close and S. Monaghan, Phys. Lett. 110B, 159 (1982).

51) T. Appelquist, R. M. Barnett and K. D. Lane, Ann. Rev. Nucl. Part. Sci. 28, 387 (1978); C. Quigg and J. L. Rosner, Phys. Rev. D 23, 2625 (1981); E. Eichten et al., Phys. Rev. D 17, 3090 (1978); E. Eichten et al., ibid, D 21, 203 (1980); W. Buchmüller and S.-H. H. Tye, Phys. Rev. D 24, 132 (1981).

52) E. Eichten and F. Feinberg, Phys. Rev. D 23, 2724 (1981); V. Novikov et al., Phys. Rep. 41C, 1 (1978); M. A. Shifman and M. I. Vysotsky, Z. Phys. C10, 131 (1980).

53) T. M. Himel et al., Phys. Rev. Lett. 45, 1146 (1980).

54) R. Partridge et al., Phys. Rev. Lett. 45, 1150 (1980).

55) R. Barbieri, R. Gatto and E. Remiddi, Phys. Lett. 61B, 465 (1976), and TH-3144-CERN (1981).

56) J. Gaiser, SLAC-PUB-2887, and Proc. of the XVIIth Rencontre de Moriond, Les Arcs, France, January 1982.

57) C. Edwards et al., Phys. Rev. Lett. 48, 70 (1982).